13 N. Aissaoui, J. Landoulsi, L. Bergaoui, S. Boujday and J. F. Lambert: Enzyme Microb. Technol. **52** (2013) 336.
14 M. Bariana, M. S. Aw, M. Kurkuri and D. Losic: Int. J. Pharm. **443** (2013) 230.
15 M. Yamada, M. Terao, T. Terashima, T. Fujiyama, Y. Kawaguchi, Y. Nabeshima and M. Hoshino: J. Neurosci. **27** (2007) 10924.
16 M. Ito: The Cerebellum and Neural Control (Raven Press, New York, 1984) Chap. 1.
17 M. L. Fiszman and A. Schousboe: J. Neurosci. Res. **76** (2004) 435.
18 K. Okochi, S. Hirano, K. Maruya, T. Morishima, C. Takayama, A. Fukuda and S. Yoshida: Neurosci. Res. **61** (2008) S114.

About the Authors

Kazunori Watanabe was born in Hokkaido, Japan, on February 3, 1992. He is a 2nd-year student in the Graduate School of Toyohashi University of Technology. His research focuses on the optimization of surface modifications for biosensors and the detection of neurotransmitters. He is a member of the Japan Neuroscience Society.

Nobuto Takahashi was born in Tokyo, Japan, on December 9, 1992. He is a 1st-year student in the Graduate School of Toyohashi University of Technology. His research focuses on bioengineering photoanalysis of cells and the developmental mechanism of cultured neurons. He is a member of the Japan Neuroscience Society.

Naohiro Hozumi was born in Kyoto, Japan, on April 2, 1957. He received his B.S., M.S., and Ph.D. degrees in 1981, 1983, and 1990, respectively, from Waseda University. He was at the Central Research Institute of Electric Power Industry (CRIEPI) from 1983 to 1999. He was an associate professor at Toyohashi University of Technology from 1999 to 2006, and a professor at Aichi Institute of Technology from 2006 to 2011. Since 2011, he has been a professor at Toyohashi University of Technology. He has been engaged mostly in research on insulating materials and diagnosis of high-voltage equipment and acoustic measurement for biological and medical applications. In 1990 and 1999, he received awards from IEE of Japan for his outstanding research papers. He is a member of IEEE, IEE of Japan, and the Acoustic Society of Japan.

Sachiko Yoshida was born in Toyama, Japan, on January 24, 1961. She received her B.S., M.S., and Ph.D. degrees in 1983, 1986, and 1990, respectively, from the University of Tokyo. She was a JSPS Postdoctoral Researcher from 1990 to 1992, a JST PRESTO Researcher from 1992 to 1994, and a research associate at Toyohashi University of Technology from 1995 to 1996. Since 1996, she has been a lecturer at Toyohashi University of Technology. Her research interests focus on physiological interaction and morphological transformation through brain differentiation, and their detection. She is a member of IEEE, International Brain Research Organization, the Society for Neuroscience, and the Japan Neuroscience Society.

電気学会論文誌 A（基礎・材料・共通部門誌）
IEEJ Transactions on Fundamentals and Materials
Vol.136 No.2 pp.99-104 DOI: 10.1541/ieejfms.136.99

Paper

Visualization of Spatially Distributed Bioactive Molecules using Enzyme-Linked Photo Assay

Hikaru Mabuchi* Student Member, HongYao Ong* Associate
Kazunori Watanabe* Non-member, Sachiko Yoshida* Non-member
Naohiro Hozumi*a) Senior Member

(Manuscript received March 18, 2015, revised Oct. 4, 2015)

In this paper, we propose a new simple device for visualizing bioactive molecules with a fine spatial resolution by using a membrane in which a specific enzyme is immobilized. The layer produces fluorescence after association with a specific substance. The layer, on which a biological tissue is to be mounted, is deposited on a quartz substrate that is used as a light guide to introduce UV light to the layer. Substance release is observed by a CCD camera from the opposite side of the substrate. In order to shorten the experiment time, we had automated the optical device. The paper also describes the reduction of background fluorescence by means of image processing technique. Images were acquired by employing two UV-LEDs with slightly different angle. Image processing was performed to separate background and target fluorescence by means of independent component analysis. Finally the release of GABA(γ-aminobutyric acid) and glutamate from specific layers in rat cerebellum was successfully observed. It is expected that, using this method, both real-time transmitter release and its response to medicine can be observed.

Keywords : bioactive molecules, enzyme-linked photo assay, independent component analysis

1. Introduction

Light guide is composed of a dielectric material that can enclose the light propagation. In addition to being applied to communication, it is useful for sensing as well. In chemical sensing the surface of the light guide has to be coated with some specific chemical that may change its optical property depending on chemical reactions. Such a function can be applied to chemical imaging, if the light guide has a flat surface. This study proposes an application of two-dimensional light guide, of which surface is chemically modified, to biochemical imaging.

Neurotransmitter molecules released from neurons are not only regulators of neuronal transduction but also indicators of neuronal conditions. Glutamate and γ-aminobutyric acid (GABA) are known as typical transmitters in brain cortex that play important roles as stimulator and suppresser, respectively. Lack of balance in the release of glutamate and GABA may lead to autism, epilepsy or Parkinson's disease[1][2].

In order to observe the spatio-temporal release in cerebellar cortex, we have newly proposed the enzyme-linked photo assay system, which is realized even using normal CCD camera, and observed GABA release in developing cerebellar slice using either new or authorized methods[3].

In this paper, we propose a new simple device for this purpose by using a reactive layer in which a specific enzyme is immobilized, and produces fluorescence after association with a specific substance released from mounted slice. This layer is bound a quartz substrate that is used as a light guide for UV light excitation. Fluorescence derived from a substance is observed by a CCD camera from the opposite side of the substrate.

The paper describes the reduction of background fluorescence by means of image processing technique. Finally it will be shown that the release of transmitters from specific layers in rat cerebellum was successfully observed.

2. Specimen Preparation and Photo Excitation System

Imaging of neurotransmitter release was monitored the reaction of oxidoreductases generating reduced nicotinamide adenine dinucleotide (NAD^+) or diphosphonucleotide ($NADP^+$). For glutamate and GABA, we used glutamate dehydrogenase and GABA disassembly enzyme (GABase), respectively.

Enzymes were covalently immobilized on the quartz glass substrate using a silane coupling agent and a crosslink agent. The substrate was as thick as 1 mm. Stoichiometrically generated NADH or NADPH emits 480 nm fluorescence after excitation at 340-365 nm.

Existence of glutamate and GABA lead to fluorescence when co-existing with specific enzyme and co-enzyme. A glass substrate on which specific enzyme is coated is in contact with the biological specimen. A chamber space is created around the specimen. The space is filled with buffer liquid and co-enzyme. On the glass substrate therefore, the specimen is in contact with both enzyme and co-enzyme.

Consequently glutamate or GABA, that is released from the tissue spontaneously by stimulation, makes an oxidation-reduction reaction on the substrate. Although both glutamate and GABA do not produce fluorescence by themselves, NAD(P)H that is created as the result of the above chemical reaction makes fluorescence. As the ratio of glutamate or GABA and NAD(P)H is 1:1, the

a) Correspondence to: Naohiro Hozumi. E-mail: hozumi@icceed.tut.ac.jp
* Toyohashi University of Technology
1-1, Hibarigaoka, Tenpaku, Toyohashi 441-8580, Japan

fluorescence can be correlated to the amount of released glutamate or GABA.

In the experiment, rat cerebellum was sliced sagittally at 400 μm thick and incubated in oxygen-aerated HEPES-Na^+ buffer for 40 min. The slice was placed on the quartz glass substrate with both $NADP^+$ and α-ketoglutarate. Figure 1 shows the schematic diagram of the observation system including the device. The enzyme was immobilized covalently on the glass as shown in Fig. 2. Figure 3 shows chemical reactions taking place on the substrate. $NADP^+$ (nicotinamide adenine dinucleotide phosphate) changes into NADPH (reduced nicotinamide adenine dinucleotide phosphate) just as glutamate and GABA degeneration. Synthesized NADPH was illuminated by 360 nm surface UV-LED, and emitted the 480 nm fluorescent light observed by cooled CCD (ORCA ER, Hamamatsu Photonics). The quartz substrate can be recognized as a light guide to illuminate the surface of the substrate.

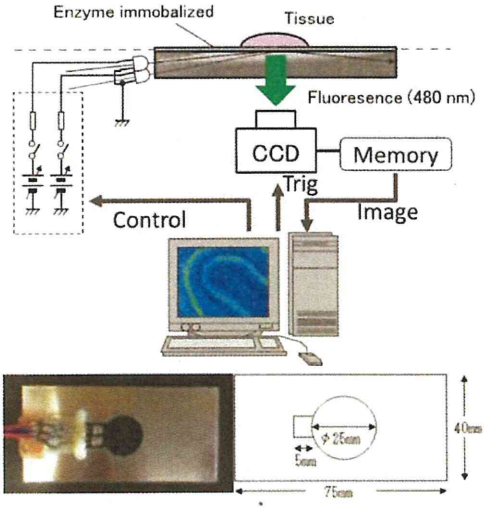

Fig. 1. Schematic diagram of the observation system including the device and its outlook

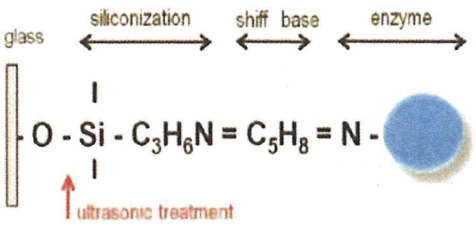

Fig. 2. Immobilized enzyme

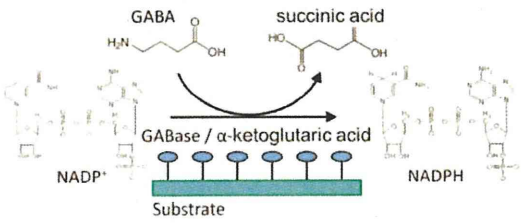

Fig. 3. Chemical reaction on the substrate

3. Image Processing

The fluorescent light detected by the CCD camera is divided into target light and background light. As significant intensity of background light is detected, it is assumed that fluorescence is excited by the light that is refracted on the interface between the substrate and tissue system including the layer. The light, being generated by LEDs and propagates though the substrate, can be decomposed into plane waves with different angles of propagation. Each plane wave transfers across the enzyme layer and comes into the tissue. We assume that both target and background light were predominantly excited by normal light. As the background light significantly damage the quality of the image, it should be reduced as much as possible. Making use of the evanescent light may be a solution, however, it may make the system complicated, and the target light may be not as significant as this case. Therefore we tried to reduce the background by means of a simple image processing.

Assuming that the light is a plane wave and scatter can be neglected, wave propagation and detected fluorescence can be illustrated as Fig. 4. In the figure, fluorescence, attributed to the layer where the enzyme is fixed, is represented as I_0. This is

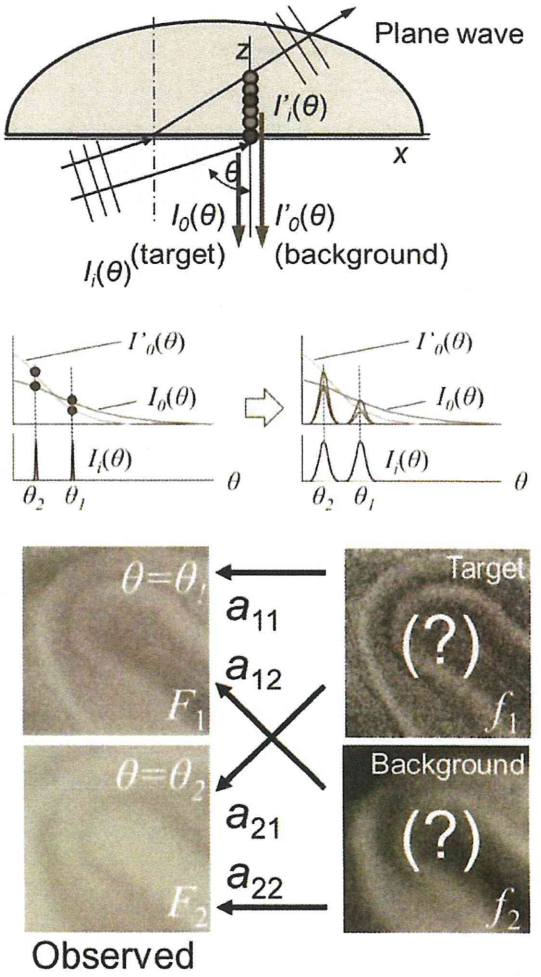

Fig. 4. Fluorescence detected by CCD camera

defined as to be the target. The fluorescence attributed to the tissue is represented as I'_0. This is defined as to be the background. Both I_0 and I'_0 depends on the incident angle θ. The thickness of the quartz plate, which is used as a light guide, is as thick as 1 mm. As it is much thicker than the diameter of normal optical fiber it is relatively easy to introduce two kinds of lights of which angles of center axes are significantly different. In addition, in practice, they depend differently on the incident angle. As the result, the proportion (I_0/I'_0) is not the same along θ. This is true even if the incident angle has distributed.

As the result, the captured fluorescence with different angle of optical axis is composed of target and background fluorescence with different mixture ratios. This can be represented as:

$$\begin{pmatrix} F_1 \\ F_2 \end{pmatrix} = \begin{pmatrix} a_{11} & a_{12} \\ a_{21} & a_{22} \end{pmatrix} \begin{pmatrix} f_1 \\ f_2 \end{pmatrix} \quad \cdots\cdots (1)$$

where $F_1(x,y)$ and $F_2(x,y)$ are captured fluorescence image, $f_1(x,y)$ and $f_2(x,y)$ are spatial distributions of fluorescence as the target and background, a_{11}, a_{12}, a_{21}, a_{22} are constants. Although the image acquisition is sequential, ICA is performed by assuming that two images, $F_1(x,y)$ and $F_2(x,y)$ are acquired with a negligible time lag. Reproduced images $f'_1(x,y)$ and $f'_2(x,y)$ are calculated from F_1 and F_2. As the result of periodical acquisitions of F_1 and F_2, time dependent images of f'_1 and f'_2 are calculated. Eq. (1) can also be described using a matrix expression as:

$$\mathbf{F} = \mathbf{A} \cdot \mathbf{f} \quad \cdots\cdots (2)$$

The target and background fluorescence distribution can be calculated by applying $\mathbf{A}^{-1}$ to $\mathbf{F}$. In practice, only contrast of the image would be enough to recognize the distribution. In such a case $\mathbf{A}^{-1}$ can be represented as:

$$\begin{pmatrix} 1 & \alpha \\ \beta & 1 \end{pmatrix} \quad \cdots\cdots (3)$$

After capturing two images $\mathbf{F}_1$ and $\mathbf{F}_2$ by changing the angle of optical axis, the target and background images can be separated by finding appropriate numbers for α and β. α and β can be tuned manually by monitoring the quality of reproduced image, however, the theory of independent component analysis (ICA) may be powerful for solving such a problem[4].

Stochastic distribution of pixel intensity in images f'_1 and f'_2 are represented as $p(y_{1i})$ and $p(y_{2j})$, where y_{1i} and y_{2j} represent the intensity.

$$\left.\begin{aligned} p(y_1) &\equiv \{p(y_{11}),\cdots,p(y_{1i}),\cdots p(y_{1n})\} \\ p(y_2) &\equiv \{p(y_{21}),\cdots,p(y_{2j}),\cdots p(y_{2n})\} \end{aligned}\right\} \quad \cdots\cdots (4)$$

$p(y_{1i},y_{2j})$ represents the probability that the intensity of a pixel in image f'_1 is y_{1i} and that of the corresponding point in image f'_2 is y_{2j}. In other words $p(y_1)$ and $p(y_2)$ are probabilities that cases y_1 and y_2 take place, respectively, and $p(y_1,y_2)$ is the probability that cases y_1 and y_2 takes place simultaneously. Variables y_1 and y_2 are considered to be independent when

$$p(y_1,y_2) = p(y_1)p(y_2) \quad \cdots\cdots (5)$$

is established. Kullback-Leibler(K-L) parameter is often employed to indicate the independency of variables:

$$KL \equiv \sum_{i,j} p(y_{1i},y_{2j}) \log \frac{p(y_{1i},y_{2j})}{p(y_{1i})p(y_{2j})} \quad \cdots\cdots (6)$$

The K-L parameter is zero when two sets of variables y_1 and y_2 are completely independent together. In practice, α and β in Eq. (3), which determine the probabilities $p(y_1)$, $p(y_2)$ and $p(y_1,y_2)$, can be tuned so that the K-L parameter indicates the minimum.

The process of ICA is illustrated in Fig. 5. The equation described in the form of matrix indicates that two images, F_1 and F_2, derive from linear combination of unknown original images f_1 and f_2. If an appropriate inverse matrix can be found then the original images can be reproduced. However as the matrix to describe the linear combination is unknown as well, ICA algorithm is applied to find the most appropriate matrix (as the inverse matrix). In the

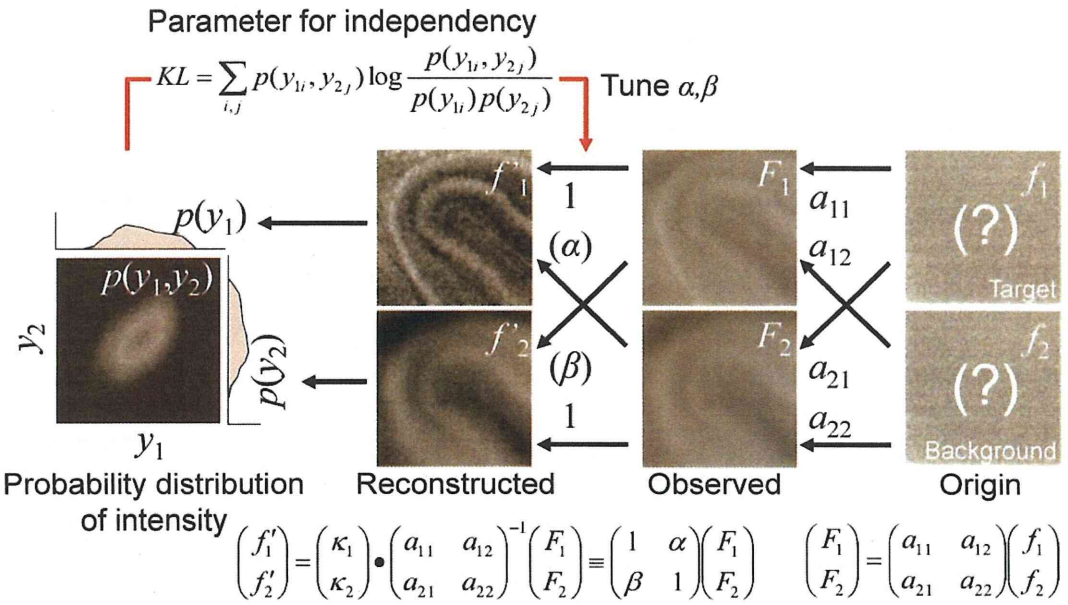

Fig. 5. Illustration for image processing based on independent component analysis

ICA process K-L parameter is calculated in order to evaluate the probabilistic independency of images f'_1 and f'_2. It can be considered that in the reproduction algorithm the core process is the calculation of the K-L parameter. In this preliminary study K-L parameter is successively calculated by manually changing the inverse matrix, and images are assumed to be reproduced when the K-L parameter indicates the minimum.

4. Results and Discussion

4.1 Image Processing using the ICA Figure 6 (a) shows visible light image of the cerebellum with postnatal 21 days. In developing cerebellum, granule cells, small input neurons, proliferate and migrate down from the external granular layer (EGL) to the internal granular layer (IGL). As the development proceeds, EGL turns into molecular layer (ML) whereas IGL remains. Purkinje cells, big output neurons, develop their dendrites and associate neuronal connections between granule cells and other interneurons. Neuronal circuit layer forms the ML. As the cerebellum shown in Fig. 6 (a) is mature, ML, PL, IGL are clearly visible. Note that ML is on the outer side of the cerebellum, and a wrinkle surrounded by the ML is seen in Fig. 6 (a).

As for fluorescence observation, three different images were acquired. Two were with different inclination of the excitation light source, and one was with no excitation light. Each of the two images with excitation light was subtracted with the image with no excitation light, in order to reduce the background light from the outside. These two images after the subtraction were defined as images A and B.

Figure 6 (b) shows these images for a rat cerebellum. Both images are very unclear, because of the background fluorescence. Figure 6 (c) shows the result of image processing. It is clearly shown in the image entitled as "target" that the fluorescence intensity is high in two layers, whereas that entitled as "background" is not clear. By morphological inspection these layers are recognized as ML and IGL. These layers are known that GABAergic neurons distribute in mature cerebellum. Studies using HPLC and electrophysiological method have shown that GABA is released from the postnatal cerebellar cortex even before synaptogenesis, and that GABA receptors act on the developing cerebellar Purkinje cells[4][5]. However, dynamic GABA release could not be observed unless the enzyme-linked photo assay is used. In addition, because cytoplasmic autofluorescence becomes noisy background light, it is useful that the image processing system extracted the image of GABA release from the autofluorescence-contained image. Using this method, both real-time transmitter release and its response to medicine can be observed.

4.2 Transition after Chemical Stimulation In relatively developed cerebellum, cells distributed in the ML and IGL are only the neurons of glutamate release, so that both layers showed fluorescent activities. Figure 7 indicates release distribution of glutamate in comparison with normal optical image illuminated with visible light. The fluorescent image, indicating glutamate release, is after the ICA processing. Figure 7 (c) indicates the regions of interest for analysis. Regions highlighted as ML and IGL have relatively strong intensity in fluorescence. They have a contrast to the region highlighted as PL. Release from white matter (WM), which is mostly composed of fatty materials, is much less significant.

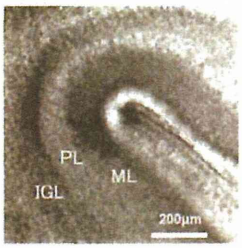

(a) Visible light image

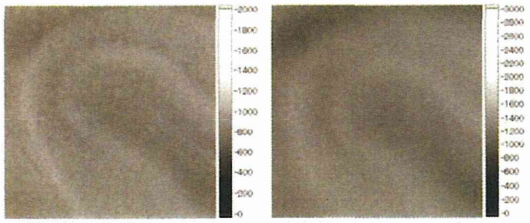

Small angle (image A). Large angle (image B).

(b) Fluorecence images before image processing

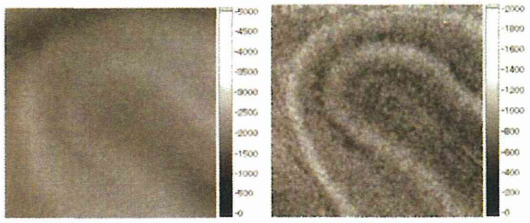

Background Target

(c) Fluorecence images after image processing

Fig. 6. Cross sectional mages of cerebellar cortex: (a) Visible light image, (b) original fluorescent images with different angle of optical axes, and (c) fluorescent images after the image processing. Scales are indicated in arbitrary unit. Specimen: rat cerebellum (postnatal 21 days), target: GABA

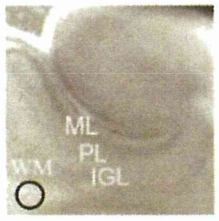

(a) Visible light image

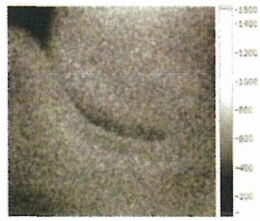

(b) Fluorescent image

(c) Regions of interest for analysis

Fig. 7. Cerebellum with postnatal 7 days observed with visible light and fluorescent light indicating glutamate release. 0.9 mm × 0.9 mm. Gray scale is arbitrary. ML: molecular layer, PL: Purkinje layer, IGL: internal granular layer, WM: white matter. Specimen: rat cerebellum (postnatal 7 days)

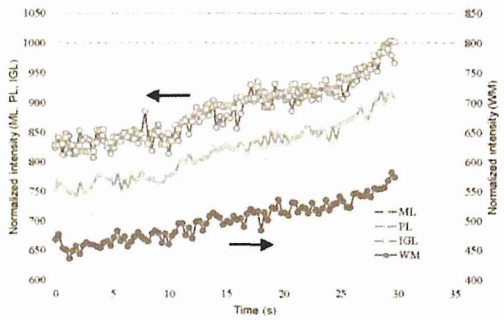

Fig. 8. Transition in fluorescence intensity in each layer (normalized by the intensity of ML 30 s after stimulation that is indicated as 1000). Specimen: rat cerebellum (postnatal 7 days), target: glutaminate

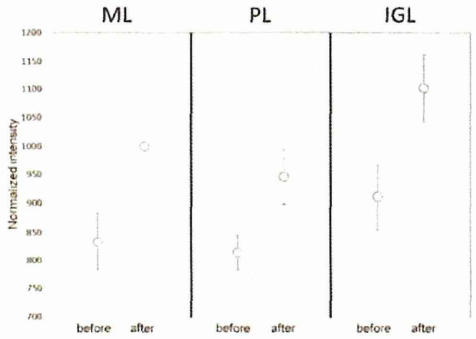

Fig. 9. Change in fluorescence intensity before and after AMPA stimulation (normalized by the intensity of ML 30 s after stimulation that is indicated as 1000). Specimen: rat cerebellum (postnatal 7 days), target: glutaminate

Our system can visualize both spontaneous and responsive transmitter release with about 0.2 s time resolution. Figure 8 shows the transition of glutamate release in response to 100 μmol/ℓ (S)-alpha-Amino-3-hydroxy- 5 methylisoxazole-4-propionic acid (AMPA) application in cerebellar slices. All values are normalized by the intensity of ML 30 s after stimulation that is indicated as 1000. Fluorescence, as indication glutamate release, was intense in both the IGL and ML, whereas the PL was indicated with lower intensity. As shown in Fig. 8, a clear increase in fluorescence was observed after stimulation. Transition in fluorescence was similar for ML and IGL, suggesting that these layers are activated. However PL, which was not expected to release glutamate, showed fluorescence as well although it was less intense than ML and IGL. As this specimen was taken from relatively young rat (postnatal 7 days), the cerebellar development was not totally completed, and the layers were not separated enough. It is hence considered that diffusion from ML and IGL to PL would take place, leading to an increase in fluorescence in this layer. The increase in fluorescence in WM suggests that glutamate might have been diffused into WM as well, although the absolute value was much lower than ML and IGL.

Figure 9 compares the fluorescence in each layer before and after stimulation. Four different specimens were used for the observation, in order to confirm reproducibility. It is clear that the AMPA stimulation brought a significant glutamate release from ML and IGL, although the increase is also seen with PL.

5. Conclusions

A new method for visualization of spatially distributed bioactive molecules using enzyme-linked photo assay has been proposed. It is based on fluorescent reaction assisted by an enzyme immobilized on the substrate, however, background fluorescence disturbs the observation. In order to reduce the background fluorescence, two images were acquired by changing the optical axis of UV illumination. Image processing based on independent component analysis made the target image clear. Observation of rat cerebellum was successfully performed and GABA and glutamate release from two specific layers was clearly indicated.

Acknowledgement

The study was partially supported by grants from Scientific Research (C) 23500516, 26350498 and Health Labor Sciences Research.

References

(1) N. C. Danbolt : "Glutamate Uptake", *Neurobiology*, Vol.65, pp.1-105 (2001)
(2) N. Kasai, Y. Jimbo, O. Niwa, T. Matsue, and K. Torimitsu : "Rea-time Multisite Observation of Glutamate Release in Rat Hippocampal Slices", *Neurosdence Lett.*, Vol.304, pp.112-116 (2001)
(3) T. Morishima, M. Uematsu, T. Furukawa, Y. Yanagawa, A. Fukuda, and S. Yoshida : "GABA Imaging in Brain Slices Using Enzyme-linked Photo Analysis", *Neurosci. Res.*, Vol.67, pp.347-353 (2001)
(4) V. Calhoun, G. Pearlson, and T. Adali : "Independent Component Analysis to fMRI Data, A Generative Model for Validating Results", VLSI Signal Processing, Vol.37, pp.281-291 (2004)
(5) F. F. Trigo, M. Chat, and A. Marty : "Enhancement of GABA Release through Endogenous Activation of Axonal GABA(A) Receptors in Juvenile Cerebellum", *J. Neurosci.*, Vol.27, No.46, pp.12452-63 (2007)
(6) K. Obata : "Excitatory and Trophic Action of GABA and Related Substances in Newborn Mice and Organotypic Cerebellar Culture", *Dev Neurosci*, Vol.19, No.1, pp.117-119 (1997)

Hikaru Mabuchi

(Student Member) was born in Hokkaido, Japan on July 25, 1992. He is 1st-year student in Graduate School of Toyohashi University of Technology. His major is electric and electronic information. He has been engaged in research on bio-sensing by means of optical measurement. He is a student member of IEEJ.

HongYao Ong

(Associate) was born in Malaysia on June 30, 1990. He received his B.S degree in 2014 from Toyohashi University of Technology, Japan. His major is electric and electronic information. He is currently engaged in GS Reality Sdn. Bhd., Malaysia. His major is electric and electronic information. He is an associate member of IEEJ.

Kazunori Watanabe

(Non-member) was born in Asahikawa, Japan on February 3, 1992. He is 2nd-year student in Graduate School of Toyohashi University of Technology. His research focuses both the optimization of surface modification for biosensor, and detection of neurotransmitters. He is a member of Japan neuroscience Society.

Sachiko Yoshida

(Non-member) was born in Toyama, Japan on January 24, 1961. She received her B.S., M.S. and Ph.D. degrees in 1983, 1986 and 1990 from University of Tokyo. She was engaged in JSPS Postdoctoral Researcher from 1990 to 1992, JST PRESTO Researcher from 1992 to 1994, and Research Associate at Toyohashi University of Technology from 1995 to 1996. Since 1996, she has been a lecturer of Toyohashi University of Technology. Her research interests focus the physiological interaction and morphological transformation through brain differentiation, and these detections. She is a member of a member of IEEE, International Brain Research Organization, Society for neuroscience, Japan neuroscience Society, and the Physiological Society of Japan.

Naohiro Hozumi

(Senior Member) was born in Kyoto, Japan on April 2, 1957. He received his B.S., M.S. and Ph.D. degrees in 1981, 1983 and 1990 from Waseda University. He was engaged in Central Research Institute of Electric Power Industry (CRIEPI) from 1983 to 1999. He was an associate professor of Toyohashi University of Technology from 1999 to 2006, and a professor of Aichi Institute of Technology from 2006 to 2011. Since 2011, he has been a professor of Toyohashi University of Technology. He has been engaged in the research in insulating materials and diagnosis for high voltage equipment, acoustic measurement for biological and medical applications, etc. He was awarded in 1990 and 1999 from IEE of Japan for his outstanding research papers. He is a member of IEEE, IEE of Japan and the Acoustic Society of Japan.

A cross-fostering analysis of bromine ion concentration in rats that inhaled 1-bromopropane vapor

Toru ISHIDAO[1], Yukiko FUETA[1], Susumu UENO[2], Yasuhiro YOSHIDA[3], and Hajime HORI[1]

[1] Department of Environmental Management, School of Health Sciences, University of Occupational and Environmental Health, Japan.

[2] Department of Occupational Toxicology, Institute of Industrial Ecological Sciences, University of Occupational and Environmental Health, Japan.

[3] Department of Immunology and Parasitology, School of Medicine, University of Occupational and Environmental Health, Japan.

Correspondence to: Toru Ishidao, Department of Environmental Management, School of Health Sciences, University of Occupational and Environmental Health, Japan. Iseigaoka 1-1, Yahatanishi-ku, Kitakyushu 807-8555, Japan

(*e-mail: ishidao@health.uoeh-u.ac.jp*)

Running title: **A cross-fostering analysis of bromine ion concentration**

The number of words in the abstract: **238**; text: **2087**, and the number of tables: **2**; figures: **3**

Field: ***Toxicology***

Abstract: Objective: Inhaled 1-bromopropane decomposes easily and releases bromine ion. However, the kinetics and transfer of bromine ion into the next generation have not been clarified. In this work, the kinetics of bromine ion transfer to the next generation was investigated by using cross-fostering analysis and a one-compartment model. **Methods:** Pregnant Wistar rats were exposed to 700 ppm of 1-bromopropane vapor for 6 h per day during gestation days (GDs) 1–20. After birth, cross-fostering was performed between mother exposure groups and mother control groups, and the pups were subdivided into the following four groups: exposure group, postnatal exposure group, gestation exposure group, and control group. Bromine ion concentrations in the brain were measured temporally. **Results:** Bromine ion concentrations in mother rats were lower than those in virgin rats, and the concentrations in fetuses were higher than those in mothers on GD20. In the postnatal period, the concentrations in the gestation exposure group decreased with time, and the biological half-life was 3.1 days. Conversely, bromine ion concentration in the postnatal exposure group increased until postnatal day 4 and then decreased. This tendency was also observed in the exposure group. A one-compartment model was applied to analyze the behavior of bromine ion concentration in the brain. By taking into account the increase of body weight and change in the bromine ion uptake rate in pups, the bromine ion concentrations in the brains of the rats could be estimated with acceptable precision.

Key words: 1-Bromopropane inhalation, Cross-fostering, Bromine ion concentration, One-compartment model, Animal experiment

1-Bromopropane (1-BP, CAS no. 106-94-5) is widely used as a substitute for chlorofluorocarbons, which destroy the ozone layer. The toxicity of 1-BP has been

reviewed[1)], and the Japan Society for Occupational Health recommends an occupation exposure limit of 0.5 ppm[2)]. Previously, we studied the effects of inhaled 1-BP vapor in male rats on the nervous[3-8)] and immune systems[9, 10)].

We also studied the effects of inhaled 1-BP vapor on metabolism in male rats and reported that 1-BP rapidly decomposes and releases bromine ion in the blood[11)], indicating that bromine ion is a major index of 1-BP exposure. Recently, because of the health effects reported in female workers exposed to 1-BP[12-14)], there is concern regarding the health effects of 1-BP exposure on the next generation. Some researchers have reported results of experiments in female animals[15-17)]; however, the kinetics of bromine ion distribution to the next generation has not been elucidated. In this study, pregnant rats were exposed to 700 ppm of 1-BP vapor, and the concentration of bromine ion in the rat brain was measured. The distribution of bromine in fetuses and cross-fostered pups was investigated. A one-compartment model was employed to analyze the behavior of bromine ion in rats.

Methods

Animals

Female (9-week-old) and male (10-week-old) Wistar rats were purchased from Kyudo Co., Ltd. (Saga, Japan). After acclimation in polycarbonate cages with dry chips, they were housed in pairs in animal rooms under 12-h light–dark cycle conditions at 22 ± 1°C and 55 ± 5% relative humidity, with free access to food and water. The presence of sperm in the vaginal smear was defined as day 0 of gestation (GD0; female rats were 11 weeks old). In the inhalation study, the female rats were divided into three groups: 1-BP-exposed virgin female group (n = 5), 1-BP-exposed mother group (n = 11), and the control mother group (n = 5). After the final exposure of mother rats on GD20, they

were housed in an animal room for the onset of birth. Postnatal day (PND) i.e., the day after birth, was defined as day 0 (PND0 = GD21). On PND1, a litter size of eight pups was assembled and cross-fostering[17, 18] of pups was performed between mother exposure groups (n = 3) and mother control groups (n = 3). The pups were subdivided into four groups: (1) exposure group (1-BP-exposed pups were raised by their birth mother exposed to 1-BP), (2) postnatal exposure group (control pups were raised by 1-BP-exposed mother), (3) gestation exposure group (1-BP-exposed pups were raised by control mother), and (4) control group (control pups were raised by their control mother). The experimental groups are summarized in Table 1. Body weight was measured periodically. The experiments were conducted per the guidance of the Ethics Committee of Animal Care and Experimentation in accordance with The Guiding Principle for Animal Care Experimentation, University of Occupational and Environmental Health, Japan (AE03-065), which conforms to the National Institutes of Health Guide for the Care and Use of Laboratory Animals and the Japanese Law for Animal Welfare and Care.

Exposure

Reagent-grade 1-BP was obtained from Kanto Chemical Co., Ltd. (Tokyo, Japan). 1-BP vapor was introduced into a 400-*l* stainless-steel exposure chamber. Details of this apparatus and procedure have been given elsewhere[11]. In order to study change in bromine ion in blood and brain when the condition of dysfunction of feedback inhibition (i.e., disinhibition) was confirmed, exposure concentration was designed to be 700 ppm, which was higher than LOAEL (400 ppm) for disinhibition[7]. The actual concentration of 1-BP vapor in the chamber was 701.3 ± 5.2 ppm. In the control group, only clean air was introduced into the chamber. The exposure period was 6 h per day

between 9 a.m. and 3 p.m. throughout gestation or GD1-20 (virgin female group was exposed until GD21). Table 1 displays the age of the rats on sampling day. They were deeply anesthetized with diethyl ether and then decapitated. The brains and the stomachs with milk from only the exposure group on PND1 were gently removed and stored in a freezer.

Measurement of bromine ion concentration

The brains (cerebrum and diencephalon) and stomachs (0.25 g) were homogenized with water (1.5 m*l*) at 0°C. The sample (1 m*l*) was dispensed into a vial, and 0.1 m*l* of dimethyl sulfate was added to convert bromine ion to methyl bromide. Then, 0.1 m*l* of an aqueous solution of isopropyl alcohol (0.5 volume percent) was added as an internal standard. The vial was heated at 50°C for 1 h. The bromine ion concentration was determined by measuring peak area of methyl bromide vapor in the headspace by using a gas chromatograph mass spectrometer (GC/MS, QP-5050; Shimadzu, Kyoto, Japan)[11].

Estimation method of bromine ion concentration

As previously described, inhaled 1-BP was metabolized and bromine ions were released. In this study, the behavior of released bromine ion concentration in the brain was analyzed by using a one-compartment model[19]. We assumed the bromine ion uptake rate, i.e., the generation rate of bromine ion, is equal to the 1-BP uptake rate because 1-BP is decomposed quickly[11] and releases bromine ion. Under this assumption, mass balance equations of bromine ion during exposure and clearance periods respectively were as follows:

$$\frac{dx}{dt} = R - kx \tag{1}$$

$$\frac{dx}{dt} = -kx \tag{2}$$

where x is the amount of bromine ion (μg); t is time (h); R is the generation rate of bromine ion (μg/h), which corresponds to the 1-BP uptake rate; and k is the excretion rate constant (1/h). From equations (1) and (2), the bromine ion concentrations C (μg/g) during exposure and clearance respectively were obtained as follows:

$$C = \frac{R}{\rho V k}\left(1 - e^{-kt}\right) \tag{3}$$

$$C = C_0 e^{-kt} \tag{4}$$

where V is the volume of the compartment (ml), ρ is the density of the compartment (g/ml), and C_0 is the initial concentration during clearance (μg/g). The excretion rate constant k is given by the biological half-life, $t_{1/2}$ (h) or $T_{1/2}$ (days).

$$k = \frac{\ln 2}{t_{1/2}(\mathrm{h})} = \frac{0.693}{T_{1/2}(\mathrm{days}) \times 24} \tag{5}$$

Experimental Results

Fig. 1 shows the change in the average body weight of mother rats exposed to 700 ppm of 1-BP up to GD20 and that of the pups after the exposure. The time, T (on the

horizontal axis), includes the GDs and PNDs. Litter sizes of exposed mothers and control mothers were 15.0 ± 2.8 and 14.9 ± 2.5 pups, respectively. The body weight of both mothers and pups increased rapidly. This tendency was also observed in the control group, and there was no significant difference between the exposure group and the control group. For the virgin female group, body weight did not change significantly (271.1 ± 17.0 g) during GD1-20.

Bromine ion concentration in the rat brain (μg/g-brain) exposed to 700 ppm of 1-BP on GDs is presented as symbols in Fig. 2. The bromine ion concentration in mother rats was lower than that in virgin rats, and the concentration in fetuses was higher than that in mothers. Fig. 3 shows changes in bromine ion concentration in pup brain for PNDs. The concentration in the gestation exposure group decreased between PND4 and PND8, whereas that in the postnatal exposure group increased from PND2 to PND4 and then decreased. This tendency was also observed in the exposure group, although the concentration on PND1 was lower than that on GD20 (fetus in Fig. 2). Specifically, the concentration in the exposure group was the highest just after birth, but decreased at PND1. The concentration then increased from PND1 to PND3, but decreased again with time. In the control pups, the bromine ion concentration was 11.2 ± 7.7 μg/g-brain on PND3.

The bromine ion concentration in pup stomachs with milk from the exposure group on PND1 was 830.6 ± 188.8 μg/g-stomach, which was about twice as much as that in the mother brain at GD20 (Fig. 2).

Discussion

The one-compartment model was applied to analyze the bromine ion concentration in the brains of virgin females, mothers, fetuses, and pups. Equations (3) and (4) have

two parameters, the excretion rate constant k and the 1-BP uptake rate R. The excretion rate constant, k, can be easily calculated from equation (5) by using the biological half-life $T_{1/2}$ (days). In our previous work[11], $T_{1/2}$ for male rats was 4.7–15.0 days in blood and 5.0–7.5 days in urine. Therefore, $T_{1/2}$ = 7.0 days was used for mothers and virgin females in this study. $T_{1/2}$ in pups was 3.1 days, obtained by experimental data. Equation (4) was applied to the data from PND1 for the exposure group and from PND4 and PND8 for the gestation exposure group as shown in Fig. 3. $T_{1/2}$ = 3.1 days was also used for fetuses. The half-lives of between GD20 for fetuses and PND1 for the exposure group were excluded from the calculation because of the time lag due to birth.

As shown in Fig. 2, the bromine ion concentration in the brains of mothers was lower than that in the brains of virgin females. A reason for this might be that the bromine ion concentration was diluted because of increasing body weight. The average body weight of pups, w (g), was expressed using the following equation (Fig. 1):

$$w = 0.00028T^{3.31} \tag{6}$$

The average body weight of mothers, W (g), was calculated as the sum of that of virgin females (ρV = 271.1 g) and of pups, w, (interpolated value for GDs):

$$W = 271.1 + 27w \tag{7}$$

where 27 is the constant, which was determined to give the best fit for the experimental data as shown in Fig. 1.

For virgin females, the uptake rate, R, of 2853 μg/h was obtained to give the best fit

of equations (3) and (4) for the experimental data on GD21 in Fig. 2. Therefore, $R/\rho V = R/W = 2853/271.1 = 10.5$ μg/(h·g) for virgin females, and $R/\rho V = 2853/(271.1 + 27w)$ for mother rats was used in equation (3). For fetuses, R (bromine ion uptake rate from mothers) was assumed to be proportional to body weight, and $R/\rho V = R/w = 22.0$ μg/(h·g) was applied, which was obtained to give the best fit for the experimental data on GD20 in Fig. 2. On PNDs, suckling (exposure to bromine ion from milk) was assumed to occur at 2-h intervals. As shown in Fig. 3, the curve of bromine ion concentration in the brains of the postnatal exposure group is convex. In addition, on PND1, the concentration in pup stomachs with milk was high, and the level was higher than that in the mother brain, as calculated using the one-compartment model (486.2 μg/g-brain). Therefore, we assume that the uptake rate R of pups is high at first and then decreases. In this work, R in the postnatal exposure group can be expressed by the following equation:

$$R = 388e^{-0.126(t-32)} \tag{8}$$

where 32 is the initial suckling (h) and 388 and 0.126 are the constants determined experimentally. The bromine ion concentration in the exposure group was calculated as the sum of the concentrations in the gestation exposure and postnatal exposure groups. Conditions of the one-compartment model and the values of parameters obtained are listed in Table 2. Solid, broken, and dotted lines in Fig. 2 indicate calculated lines for fetuses, mothers, and virgin females, respectively. In Fig. 3, solid, broken, and dotted lines indicate calculated lines of exposure, postnatal exposure, and gestation exposure groups, respectively. The lines calculated using the proposed model could be estimated from the experimental data with acceptable precision as shown in both figures.

The calculated bromine ion uptake rates per weight, $R/\rho V$, for adults and fetuses were 10.5 and 22 μg/(h·g), respectively. This result suggests that the bromine ion easily transfers from mothers to fetuses, and the concentration in fetuses was higher than that in mothers. R in postnatal exposure group was expressed as an exponential function, and $R/\rho V$ of 55 μg/(h·g) was obtained at initial suckling time. This value was large compared to 22 μg/(h·g), the calculated value at GD20, before birth. This suggests that uptake rate of bromine ion via milk was higher than that via the placenta, and the bromine ion concentration in the exposure group could be explained as the sum of that in the gestation and postnatal exposure groups, which is shown in Fig. 3.

In summary, the results of this study suggest (1) the concentration of bromine ion in mother rats was lower than that in virgin female rats, (2) bromine ion easily transferred from mothers to fetuses and accumulated before birth, (3) bromine ion was concentrated more in milk than in the brains of the mothers, and (4) bromine ion uptake rate in pups was high immediately after birth.

Acknowledgments:

The authors thank Ms. Tomoko Tanaka, Kana Hayashi, Erika Ito, and Ai Kanemaru for technical help and Dr. Sumiyo Ishimatsu for her critical comments on our experiments.

References

1) Ichihara G. Neuro-reproductive toxicities of 1-bromopropane and 2-bromopropane. Int Arch Occup Environ Health 2005; 78; 79-96.

2) The Japan Society for Occupational Health. Recommendation of occupational exposure limits (2013-14). J Occup Health 2013; 55; 422-41.

3) Ohnishi A, Ishidao T, Kasai T, Arashidani K, Hori H. Neurotoxicity of 1-bromopropane in rats. J UOEH 1999; 21; 23-8.

4) Fueta Y, Ishidao T, Kasai T, Hori H, Arashidani K. Decreased paired-pulse inhibition in the dentate gyrus of the brain in rats exposed to 1-bromopropane vapor. J Occup Health 2000; 42; 149-51.

5) Fueta Y, Ishidao T, Arashidani K, Endo Y, Hori H. Hyperexcitability of the hippocampal CA1 and the dentate gyrus in rats subchronically exposed to a substitute for chlorofluorocarbons, 1-bromopropane vapor. J Occup Health 2002; 44; 156-65.

6) Fueta Y, Fukuda T, Ishidao T, Hori H. Electrophysiology and immunohistochemistry in the hippocampal CA1 and the dentate gyrus of rats chronically exposed to 1-bromopropane, a substitute for specific chlorofluorocarbons. Neuroscience 2004; 124; 593-603.

7) Fueta Y, Ishidao T, Ueno S, Yoshida Y, Kunugita N, Hori H. New approach to risk assessment of central neurotoxicity induced by 1-bromopropane using animal models. Neurotoxicology 2007; 28; 270-3.

8) Ueno S, Yoshida Y, Fueta Y, Ishidao T, Liu JQ, Kunugita N, Yanagihara N, Hori H. Changes in the function of the inhibitory neurotransmitter system in the rat brain following subchronic inhalation exposure to 1-bromopropane. Neurotoxicology 2007; 28; 415-20.

9) Yoshida Y, Liu JQ, Nakano Y, Ueno S, Fueta Y, Ishidao T, Kunugita N, Yamashita U, Hori H. 1-BP inhibits NF-kB activity and Bcl-xL expression in astrocytes in vitro and reduces Bcl-xL expression in the brains of rats in vivo. Neurotoxicology 2007; 28; 381-6.

10) Yoshida Y, Nakano Y, Ueno S, Liu JQ, Fueta Y, Ishidao T, Kunugita N, Yanagihara N, Sugiura T, Yamashita U, Hori H. Effects of 1-bromopropane, a substitute for chlorofluorocarbons, on brain-derived neurotrophic factor (BDNF) expression. Int Immunopharmacol 2009; 9; 433-8.

11) Ishidao T, Kunugita N, Fueta Y, Arashidani K, Hori H. Effects of inhaled 1-bromopropane vapor on rat metabolism. Toxicol Lett 2002; 134; 237-43.

12) Ichihara G, Miller JK, Ziolkowska A, Itohara S, Takeuchi Y. Neurological disorders in three workers exposed to 1-bromopropane. J Occup Health 2002; 44; 1-7.

13) Ichihara G, Li W, Ding X, Peng S, Yu X, Shibata E, Yamada T, Wang H, Itohara S, Kanno S, Sakai K, Ito H, Kanefusa K, Takeuchi Y. A survey on exposure level, health status, and biomarkers in workers exposed to 1-bromopropane. Am J Ind Med 2004; 45; 63-75.

14) Li W, Shibata E, Zhou Z, Ichihara S, Wang H, Wang Q, Li J, Zhang L, Wakai K, Takeuchi Y, Ding X, Ichihara G. Dose-dependent neurologic abnormalities in workers exposed to 1-bromopropane. J Occup Environ Med 2010; 52; 769-77.

15) Sekiguchi S, Suda M, Zhai YL, Honma T. Effects of 1-bromopropane, 2-bromopropane, and 1,2-dichloropropane on the estrous cycle and ovulation in F344 rats. Toxicol Lett 2002; 126; 41-9.

16) Yamada T, Ichihara G, Wang H, Yu X, Maeda K, Tsukamura H, Kamijima M, Nakajima T, Takeuchi Y. Exposure to 1-bromopropane causes ovarian dysfunction in rats. Toxicol Sci 2003; 71; 96-103.

17) Furuhashi K, Kitoh J, Tsukamura H, Maeda K, Wang H, Li W, Ichihara S, Nakajima T, Ichihara G. Effects of exposure of rat dams to 1-bromopropane during pregnancy and lactation on growth and sexual maturation of their offspring. Toxicology 2006; 224; 219-28.

18) Lau C, Thibodeaux JR, Hanson RG, Rogers JM, Grey BE, Stanton ME, Butenhoff JL, Stevenson LA. Exposure to perfluorooctane sulfonate during pregnancy in rat and mouse. II: postnatal evaluation. Toxicological Sci 2003; 74; 382-92.

19) Hori H, Hyakudo T, Oyabu T, Ishimatsu S, Yamato H, Tanaka I. Effects of inhaled methyl bromide gas on the metabolic system and kinetics of bromine ion in rats. J UOEH 2002; 24; 151-60.